



## OPEN Integrative bioinformatics and immunohistochemical analysis unravel the prognostic significance and immunological implication of LIMCH1 in breast cancer: a retrospective study

Xin Yu<sup>1,5</sup>, Bei Li<sup>2,5</sup>, Wenge Li<sup>3,5</sup>, Jingping Yuan<sup>2</sup>✉, Shengrong Sun<sup>1</sup>✉ & Juanjuan Li<sup>1,4</sup>✉

The current mortality rates for breast cancer underscore the need for better prognostic tools; moreover, LIM and calponin homology domain 1 (LIMCH1), which is a protein with dual roles in cancer, is a promising candidate for investigation. This study employed an integrative approach combining bioinformatics analysis of The Cancer Genome Atlas (TCGA) cohort and clinical immunohistochemistry (IHC) cohort data. We analysed LIMCH1 expression patterns, its associations with clinicopathological features and prognosis, and its impact on the tumour immune microenvironment (TIME). Functional annotations and single-cell RNA sequencing (scRNA-seq) data were used to explore the underlying molecular mechanisms. Our analysis revealed that high LIMCH1 expression in breast cancer patients was significantly associated with unfavourable clinical outcomes and served as an independent prognostic indicator. The functional annotations revealed pathways related to carcinogenesis and metabolic reconfiguration, thus suggesting the role of LIMCH1 in tumour progression. Additionally, LIMCH1 expression was correlated with an immunosuppressive TIME characterized by increased numbers of M2 macrophages and reduced numbers of CD8<sup>+</sup> T cells and NK cells. Finally, we developed a nomogram incorporating LIMCH1 expression for predicting overall survival rates, thus providing a clinically applicable tool. Our research elucidates the diverse functions of LIMCH1 in the pathogenesis of breast cancer, thus highlighting its potential utility as both a prognostic indicator and a therapeutic intervention.

**Keywords** Breast cancer, LIMCH1, Bioinformatics, Tumour immunity, Therapeutic target

### Abbreviations

BP	Biological process
CAFs	Cancer-associated fibroblasts
CC	Cellular component
DEGs	Differentially expressed genes
DFS	Disease-free survival
ECM	Extracellular matrix
FC	Fold change
GO	Gene Ontology
GSEA	Gene set enrichment analysis
GSVA	Gene set variation analysis

<sup>1</sup>Department of Breast and Thyroid Surgery, Renmin Hospital of Wuhan University, 238 Ziyang Road, Wuhan 430060, Hubei, People's Republic of China. <sup>2</sup>Department of Pathology, Renmin Hospital of Wuhan University, 238 Ziyang Road, Wuhan 430060, Hubei, People's Republic of China. <sup>3</sup>Department of Oncology, Shanghai Artemed Hospital, Shanghai, People's Republic of China. <sup>4</sup>Department of general surgery, Taikang Tongji (Wuhan) Hospital, Wuhan 430050, Hubei, People's Republic of China. <sup>5</sup>Xin Yu, Bei Li and Wenge Li contributed equally to this work. ✉email: yuanjingping@whu.edu.cn; sun137@sina.com; snowy1150219@sina.com

HUWE1	HECT, UBA, and WWE domain-containing protein 1
IC50	Half-maximal inhibitory concentration
IHC	Immunohistochemistry
KEGG	Kyoto Encyclopedia of Genes and Genomes
LIMCH1	LIM and calponin homology domains 1
MAF	Mutation annotation format
MDSC	Myeloid-derived suppressor cell
MF	Molecular function
MsigDB	Molecular signatures database
NMIIA	Non-muscle myosin IIA
OS	Overall survival
RFS	Recurrence-free survival
RNA-seq	RNA sequencing
scRNA-seq	Single-cell RNA-seq
TCGA	The Cancer Genome Atlas
TIME	Tumour immune microenvironment
TNM	Tumour, node, and metastasis

Breast cancer is a prevalent malignancy worldwide and poses a substantial threat to women's health<sup>1</sup>. Despite notable advancements in breast cancer diagnosis and treatment, a considerable cohort of patients exhibit resistance to therapy or experience relapse posttreatment. Hence, there is a pressing need to enhance existing diagnostic and therapeutic approaches. The determination of treatment strategies and prognostic assessments in patients with breast cancer predominantly relies on the tumour, node, and metastasis (TNM) staging system, in addition to molecular subtyping. Nonetheless, clinical outcomes exhibit considerable variability, even among patients with identical tumour stages and molecular subtypes who are receiving analogous treatment regimens<sup>2</sup>. This scenario implies deficiencies in the existing staging framework, which inadequately anticipates prognosis and neglects the inherent biological diversity that is observed among individuals with breast cancer. The investigation of the intrinsic attributes of both tumour cells and patients as prognostic indicators has the potential to augment the TNM staging system, thus resulting in more precise prognostic forecasts, personalized therapeutic approaches, and the advancement of novel strategies for treating breast cancer<sup>1,3</sup>.

LIM and calponin homology domain 1 (LIMCH1) has emerged as being a promising candidate for investigation in breast cancer<sup>4</sup>. This protein has been implicated in a variety of cellular processes, including cytoskeletal organization, cell motility, and signal transduction<sup>5–7</sup>. Its involvement in cellular dynamics raises the possibility of a significant impact being exerted on cancer progression. However, observations regarding the role of LIMCH1 in tumours have been contradictory. Preliminary investigations have indicated that this molecule functions as a lung cancer suppressor through its association with HUWE1 (HECT, UBA, and WWE domain-containing protein 1), which is pivotal for preserving the integrity of p53. This interaction is crucial for curbing the proliferation of lung cancer cells and diminishing tumour progression<sup>6</sup>. Concurrently, studies have suggested that LIMCH1 may contribute to the regulation of the Notch/Wnt signalling pathways, thus further modulating cell cycle regulation; moreover, it has been implicated in the specific oncogenesis of renal and lung adenocarcinomas<sup>8–10</sup>. Despite these findings, a research gap exists regarding the role of LIMCH1 in breast cancer. In the context of lung cancer research, a significant correlation with improved patient outcomes has been observed in the presence of the LIMCH1 protein<sup>7</sup>. Conversely, this protein has been implicated in adverse prognostic indicators in the context of cervical and breast cancers<sup>4,11</sup>. This dual function underscores the need for a more nuanced understanding of the role of LIMCH1 in breast cancer. The present study aims to address this knowledge gap by investigating the specific mechanisms through which LIMCH1 influences breast cancer progression and outcomes.

The advent of bioinformatics has revolutionized the discovery of biomarkers and the elucidation of their clinical significance in cancer<sup>12–14</sup>. Bioinformatics tools can elucidate the complex roles of proteins such as LIMCH1, whereby these tools integrate data from various sources to provide a comprehensive view of the functions of these proteins in cancer biology. This study used bioinformatics to explore the contradictory roles of LIMCH1 and to clarify its association with the clinical prognosis of patients with breast cancer. This investigation sought to elucidate the correlation between the expression of LIMCH1 and its clinicopathological and prognostic significance in breast cancer. Utilizing an integrative methodology that combines analyses of bulk RNA sequencing (RNA-seq) and single-cell RNA-seq (scRNA-seq), we aimed to determine the molecular mechanisms underlying the influence of LIMCH1 and investigate its connection with immune cell infiltration. Additionally, immunohistochemistry (IHC) analysis was conducted to validate this association, thereby confirming that elevated LIMCH1 expression in breast cancer patients corresponds to unfavourable outcomes. By integrating bioinformatics analysis with clinical data, we aimed to elucidate the correlations between LIMCH1 expression and clinicopathological features, prognostic significance, and immunological implications in breast cancer. This integrative approach will not only address the research gap regarding the role of LIMCH1 but also provide insights into potential therapeutic targets for this condition, thus contributing to the development of personalized treatment strategies and improved prognostic assessments for breast cancer patients.

## Materials and methods

### Differential expression analysis of LIMCH1 across cancer types

The Sangerbox 3.0 online server<sup>15</sup> was used to compute the differential gene expression between normal and tumour samples across various cancers. The raw data were sourced from the UCSC Xena Browser (<https://xenabrowser.net/>), from which a uniformly normalized pancancer dataset was downloaded, which encompassed

The Cancer Genome Atlas (TCGA), TARGET, and GTEx projects. A *t* test was used to determine the statistical significance of differential gene expression.

## Patients and specimens

### TCGA-BRCA cohort

The cohort comprised 1,091 individuals who were diagnosed with breast cancer. The RNA sequencing data, in conjunction with the clinical histories of the individuals, were procured from TCGA through the Xena data hub. Subsequent to acquisition, somatic mutation information was isolated with the assistance of the TCGAbiolinks R package. These data were then converted into the Mutation Annotation Format (MAF) utilizing the maftools R package in preparation for further analytical procedures.

### IHC cohort

Data from a cohort of 100 female patients who were diagnosed with breast cancer at Renmin Hospital of Wuhan University, which encompassed the time period from February 2015 to August 2018, were retrospectively collected from formalin-fixed, paraffin-embedded samples. This cohort included 24 patients with luminal A subtypes, 33 with luminal B subtypes, 27 with HER2-enriched subtypes, and 16 with basal-like subtypes. Only individuals with a minimum follow-up duration of 5 years were eligible for inclusion in this retrospective investigation. All of the participants provided written informed consent, and this investigation had received approval from the Institutional Ethics Committee of Renmin Hospital at Wuhan University (No. WDRY2021-KS009). All methods were performed in accordance with the relevant guidelines and regulations. The endpoint of the investigation was defined as the occurrence of either recurrence or distant metastasis.

In the respective cohorts, individuals were segregated into subsets based on LIMCH1 expression, including a high-expression subset and a low-expression subset, with the differentiation criterion being the median expression value.

## IHC

In accordance with the procedures described in our previous research<sup>16,17</sup>, IHC staining was meticulously conducted via a series of standardized procedures. Initially, tissue sections were deparaffinized, followed by antigen retrieval to enhance antibody binding. Endogenous peroxidase activity was neutralized to prevent background staining, which involved treating the samples with a 3% hydrogen peroxide solution at room temperature for 25 min while protecting them from light exposure. Nonspecific binding was subsequently blocked via incubation with 3% bovine serum albumin solution for 30 min at room temperature. The primary antibody against LIMCH1 (Abcam, ab96178, diluted 1:200, the antibody has been reported in the past to specifically detect the LIMCH1 protein by IHC<sup>18</sup>) was applied, and the samples were incubated overnight at 4 °C to allow for antibody-antigen interactions. Afterwards, the sections were incubated with horseradish peroxidase (HRP) for 50 min at room temperature to amplify the signal. The chromogenic substrate diaminobenzidine (DAB) was then applied to visualize the staining, with careful microscopic observations being performed to ensure optimal development. To highlight the cell nuclei, the sections were briefly counterstained with haematoxylin for approximately 3 min. The staining outcome was evaluated by assessing both the quantity and the intensity of the positively stained neoplastic cells. Protein expression was graded on a scale of 0 to 3, in which 0 indicated no staining, 1 represented weak staining (light brown), 2 corresponded to moderate staining (brown), and 3 denoted strong staining (dark brown). The final staining score was determined by multiplying the percentage of the stained cells by the staining intensity, thus yielding an overall score that quantified the protein expression levels.

## Calculation of gene signature enrichment scores

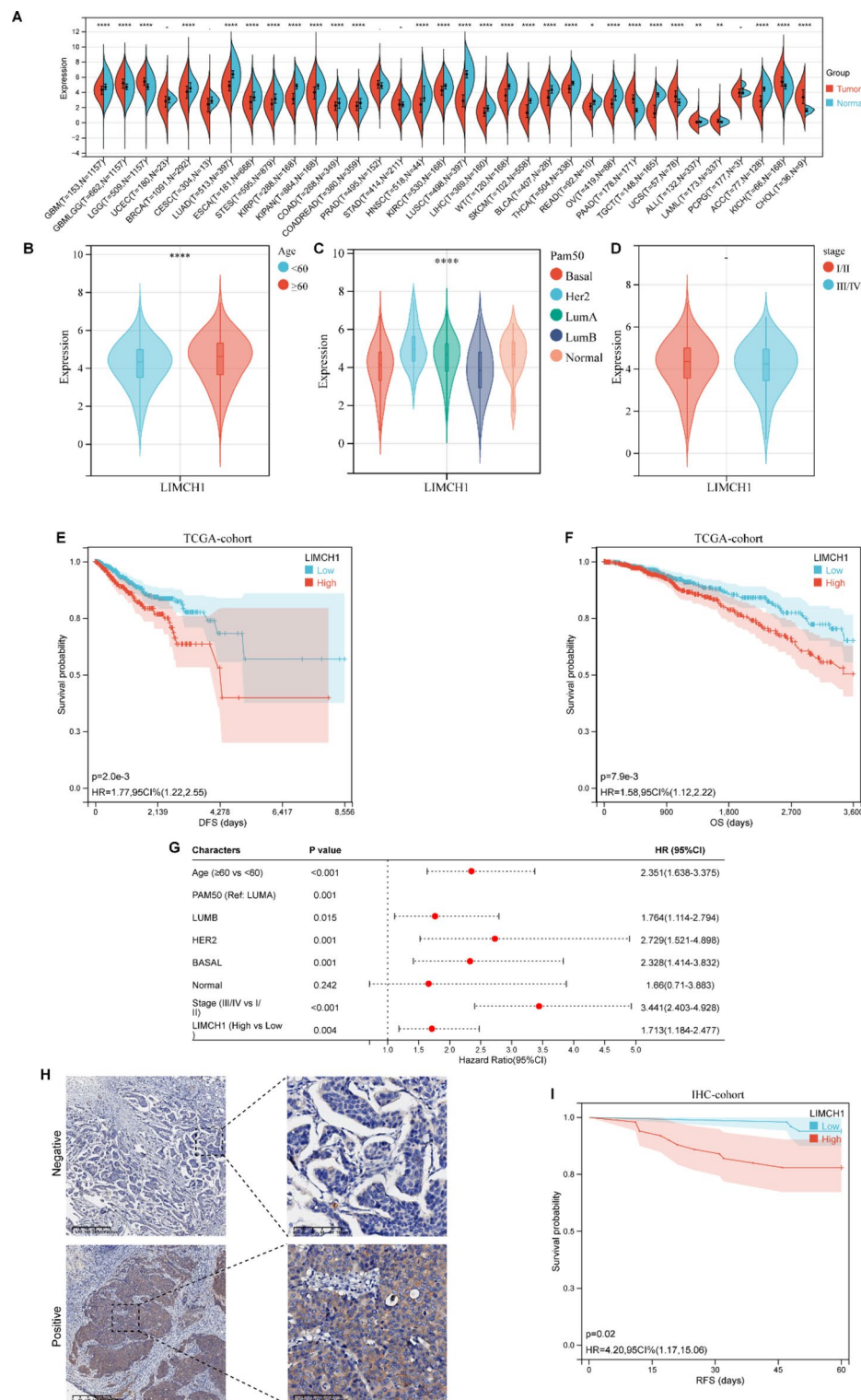
We utilized the Gene Set Variation Analysis (GSVA)<sup>19</sup> to predict the activity of specific pathways, as has been previously reported<sup>20,21</sup>. A comprehensive collection of gene signatures that are pertinent to oncological research was compiled, including metabolic gene sets from the Kyoto Encyclopedia of Genes and Genomes (KEGG) database within the Molecular Signatures Database (MSigDB), as well as gene signatures associated with drug responses. These signatures extend to pathways that are modulated by the immune system and those pathways that are indicative of a patient's potential sensitivity to radiotherapy. A detailed list of all of the gene sets is provided in Supplementary Table S1. Furthermore, the quantification of tumour-associated pathway scores across various samples was facilitated by using PROGENy software.

## Identification and annotation of differentially expressed genes (DEGs)

Utilizing the Limma R package, we identified DEGs by applying stringent criteria, including a *p* value threshold of less than 0.05 and a fold change (FC) exceeding 1.5 for both upregulated and downregulated genes. This approach facilitated the detection of genes with significant alterations in expression. The ClusterProfiler R package was subsequently used to annotate the DEGs with functional categories via Gene Ontology (GO) and KEGG pathway enrichment analyses. In parallel, gene set enrichment analysis (GSEA) was performed with ClusterProfiler, which highlighted the enrichment of significant GO, KEGG, and hallmark gene sets. This comprehensive analysis provided a robust framework for understanding the biological implications of the identified DEGs.

## Assessment of immune cell infiltration

To investigate the immunological landscape, we employed the CIBERSORT algorithm, which is an analytical method developed for the assessment of the proportions of 22 individual immune cell populations in tumour specimens. Concurrently, gene profiles associated with the cancer-immunity cycle were derived from the study



by Xu et al.<sup>22</sup>, and their enrichment levels were quantified through the application of the GSVA approach. This methodology facilitated the measurement of gene activity associated with diverse phases of the cancer immunity cycle in individual samples.

### Analysis of scRNA-seq data

In this study, we employed scRNA-seq data, which include annotations for cell clusters, in conjunction with paired bulk RNA-seq data sourced from the GEO database (GSE176078), which encompasses 24 breast tumour samples. Unsupervised clustering of individual cells was accomplished via the Seurat R package. To guarantee the integrity of the scRNA-seq dataset, we implemented quality control measures, as previously described<sup>20,23</sup>. Additionally, we conducted an analysis focusing on intercellular communication networks by utilizing the iTalk R package.



◀ **Fig. 1.** LIMCH1 transcriptional profile and prognostic significance in breast cancer. **(A)** Comparative analysis of LIMCH1 transcriptional expression in 34 cancer types and their corresponding normal tissue samples from TCGA, TARGET, and GTEx projects. *ACC* adrenocortical carcinoma, *BLCA* bladder urothelial carcinoma, *BRCA* breast invasive carcinoma, *CESC* cervical squamous cell carcinoma and endocervical adenocarcinoma, *CHOL* cholangiocarcinoma, *COAD* colon adenocarcinoma, *COADREAD* colon adenocarcinoma/rectum adenocarcinoma esophageal carcinoma, *DLBC* Lymphoid Neoplasm Diffuse Large B-cell Lymphoma, *ESCA* esophageal carcinoma, *FPPP* FFPE Pilot Phase II, *GBM* glioblastoma multiforme, *GBMLGG* glioma, *HNSC* head and neck squamous cell carcinoma, *KICH* kidney chromophobe, *KIPAN* pan-kidney cohort (KICH + KIRC + KIRP), *KIRC* kidney renal clear cell carcinoma, *KIRP* kidney renal papillary cell carcinoma, *LAML* acute myeloid leukemia, *LGG* brain lower grade glioma, *LIHC* liver hepatocellular carcinoma, *LUAD* lung adenocarcinoma, *LUSC* lung squamous cell carcinoma, *MESO* mesothelioma, *OV* ovarian serous cystadenocarcinoma, *PAAD* pancreatic adenocarcinoma, *PCPG* pheochromocytoma and paraganglioma, *PRAD* prostate adenocarcinoma, *READ* rectum adenocarcinoma, *SARC* sarcoma, *STAD* stomach adenocarcinoma, *SKCM* skin cutaneous melanoma, *STES* stomach and esophageal carcinoma, *TGCT* testicular germ cell tumors, *THCA* thyroid carcinoma, *THYM* thymoma, *UCEC* uterine corpus endometrial carcinoma, *UCS* uterine carcinosarcoma, *UVM* uveal melanoma, *OS* osteosarcoma, *ALL* acute lymphoblastic leukemia, *NB* neuroblastoma, *WT* high-risk wilms tumor. **(B–D)** Transcriptional expression of LIMCH1 stratified by **(B)** Age, **(C)** Pam50 subtypes, and **(D)** stage. **(E, F)** Kaplan–Meier analyses evaluating the prognostic value of LIMCH1 in DFS and OS using TCGA-cohort data. **(G)** Cox regression analyses evaluating the prognostic value of LIMCH1 in OS using TCGA-cohort data. **(H)** Representative immunofluorescence staining images illustrating LIMCH1 expression. **(I)** RFS curves for LIMCH1 in the IHC-cohort. Statistical significance denoted as \* $p < 0.05$ , \*\* $p < 0.01$ , \*\*\* $p < 0.001$ , \*\*\*\* $p < 0.0001$ .

### Prediction of chemotherapy response

The determination of the half-maximal inhibitory concentration (IC<sub>50</sub>) for prevalent chemotherapeutic agents was conducted via the “pRRophetic” R package.

### Development of a nomogram associated with LIMCH1

To identify potential autonomous prognostic indicators, multivariate Cox analysis was performed on LIMCH1 expression and clinical variables. Using regplot software, we subsequently constructed a nomogram linked to LIMCH1, which included age, stage, Pam50 subtype, and LIMCH1 expression as variables, to estimate survival probabilities for breast cancer patients.

### Statistical analysis

To investigate the interrelations among diverse variables, we employed Pearson correlation analysis. For continuous variables adhering to a normal distribution, a t test was used to compare these variables within binary cohorts. To further bolster the reliability of our analysis, we conducted an additional power analysis on the t tests for gene signature enrichment scores via the pwr R package. A statistical power value > 0.95 and a p value < 0.05 were considered to indicate reliability. Statistically significant differences within the subgroups of each dataset were examined via the log-rank test, and survival curves were generated via the Kaplan–Meier (KM) method. SangerBox<sup>15</sup> and R 4.0.0 were utilized for all of the statistical analyses. The obtained p values were two-tailed, with significance levels set at less than 0.05.

## Results

### Expression of LIMCH1 in breast cancer

In this study, we initially performed an analysis of LIMCH1 expression across 34 types of cancer and their corresponding normal tissues via data from the TCGA, TARGET, and GTEx databases (Fig. 1A). The results revealed significant upregulation of LIMCH1 in seven types of tumours, whereas notable downregulation was observed in 22 tumour types, including breast cancer. We subsequently explored the correlation between LIMCH1 expression and the clinical characteristics of patients with breast cancer. Interestingly, LIMCH1 was more highly expressed in older patients (Fig. 1B). In this study, we further stratified breast cancer patients based on molecular subtypes and observed that LIMCH1 expression was highest in the HER2-enriched subtype and lowest in the basal-like subtype (Fig. 1C). Additionally, LIMCH1 expression was not significantly different among patients with different stages of breast cancer (Fig. 1D).

To assess the prognostic significance of LIMCH1, we stratified patients from the TCGA cohort based on the median expression level of LIMCH1, thereby segregating them into high and low expression groups. Patients with elevated LIMCH1 expression exhibited significantly poorer disease-free survival (DFS) and overall survival (OS) (Fig. 1E, F). In the context of breast cancer research, LIMCH1 has emerged as being a significant independent predictor of prognosis, as confirmed via the application of multivariate Cox regression analysis (Fig. 1G). Subsequent prognostic analyses within the TCGA cohort (stratified by molecular subtype and clinical stage) revealed that elevated LIMCH1 expression was consistently associated with adverse outcomes in patients who were classified into the luminal A and basal subtypes, whereas no significant correlation with prognosis was observed for the other molecular subtypes (Fig. S1A–E). Moreover, increased LIMCH1 expression was uniformly correlated with poor prognosis across different clinical stages (Fig. S1F, G).

To validate our findings, we performed IHC on tissue sections from 100 breast cancer patients and confirmed that LIMCH1 was primarily expressed in epithelial cells and exhibited a diffuse cytoplasmic distribution (Fig. 1H). Consistently, elevated LIMCH1 expression was correlated with decreased recurrence-free survival

(RFS) in the IHC cohort (Fig. 1I). These results suggest that LIMCH1 may serve as a prognostic biomarker in breast cancer.

# Identification of DEGs and functional annotations

Upon identification of the DEGs, we observed that 589 genes were upregulated, whereas 42 genes were downregulated, in the high LIMCH1 expression group (Supplementary Fig. S2A, B). To gain more in-depth insights into the biological functions of these DEGs, we performed pathway analysis. The results revealed that the DEGs were predominantly associated with the “PI3K-Akt signalling pathway”, “human papillomavirus infection” and “focal adhesion” within the KEGG pathways (Fig. 2A). GO analysis revealed significant enrichment of these genes in processes such as “extracellular structure organization”, “extracellular matrix organization” and “multicellular organismal homeostasis” in the biological process (BP) category (Fig. 2B); “extracellular matrix”, “collagen-containing extracellular matrix” and “adherens junction” in the cellular component (CC) category (Fig. 2C); and “extracellular matrix structural constituent”, “cell adhesion molecule binding” and “glycosaminoglycan binding” in the molecular function (MF) category (Fig. 2D).

To further explore the connection between LIMCH1 and breast cancer, GSEA was conducted. The results revealed that patients with elevated LIMCH1 expression exhibited increased enrichment of hallmark pathways such as “fatty acid metabolism”, “haem metabolism” and “adipogenesis” (Fig. S3A-C), as well as KEGG gene sets

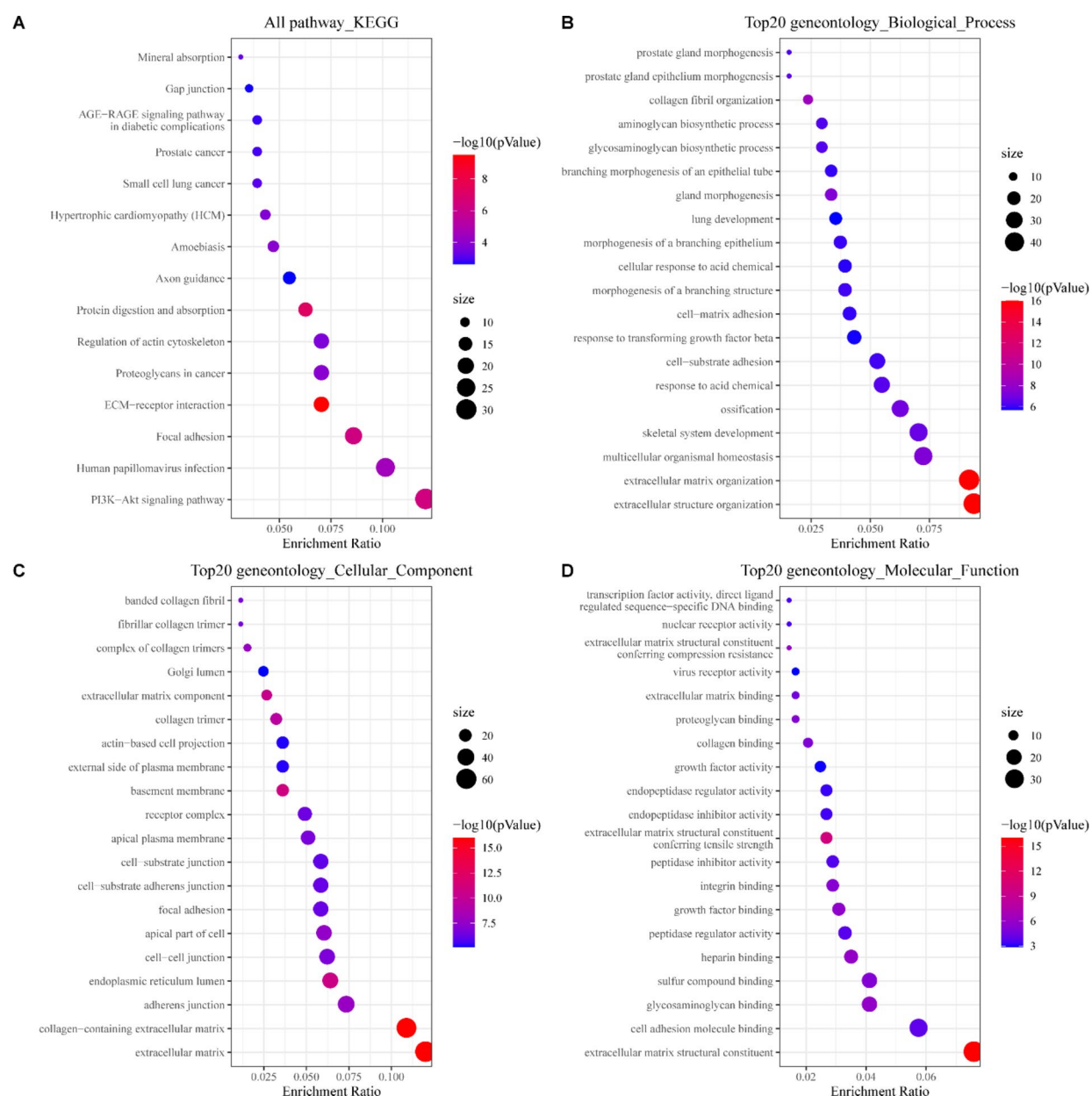


**Fig. 2.** Functional annotation of LIMCH1. Enrichment analysis of DEGs in (A) KEGG, (B) GO-BP, (C) GO-CC, and (D) GO-MF.

such as “propanoate metabolism”, “PPAR signalling pathway” and “valine leucine and isoleucine degradation” (Fig. S3D-F). Additionally, GO gene sets such as “monocarboxylic acid metabolic process”, “regulation of cell substrate adhesion” and “cell morphogenesis involved in neuron differentiation” were enriched in patients with elevated LIMCH1 expression (Fig. S3G-I). These findings collectively suggest a significant role for LIMCH1 in the carcinogenic processes associated with breast cancer.

### Association of LIMCH1 with carcinogenic pathways and gene mutations

We subsequently explored the associations between LIMCH1 and the carcinogenic pathways that are implicated in breast cancer. Our findings revealed that a majority of the carcinogenic pathways, including the androgen, EGFR, hypoxia, MAPK, NF- $\kappa$ B, p53, PI3K, TGF $\beta$ , TNF $\alpha$ , and Wnt pathways, were upregulated in the high LIMCH1 expression group (Fig. 3A, B).

Mutation site analyses revealed LIMCH1 mutations in 24 out of 34 cancer types, with mutation frequencies ranging from 0.2 to 5.1% (Fig. 3C). Notably, in breast cancer, the mutation frequency of LIMCH1 was 0.5%, which exclusively comprised missense mutations. Mutation profile analysis revealed an increased overall mutation frequency in the high LIMCH1 expression group, with PIK3CA, CDH1, and GATA3 identified as being the three most significantly altered genes. Notably, the high LIMCH1 subgroup demonstrated higher mutation frequencies for PIK3CA and GATA3, whereas CDH1 exhibited elevated mutation frequencies in the low LIMCH1 subgroup (Fig. 3D).

### Correlations between LIMCH1 and metabolism pathways

We subsequently investigated the associations between LIMCH1 and metabolic pathways (Fig. 4). Our investigation revealed a substantial correlation between elevated LIMCH1 expression and increased metabolic activity. Among the 70 KEGG metabolic pathways that were examined, 56 pathways were upregulated, whereas 2 were downregulated, in individuals with elevated LIMCH1 levels. Additionally, subjects exhibiting increased LIMCH1 expression displayed increased activation of glycolysis, the pentose phosphate pathway, and nucleotide metabolic processes. These metabolic pathways are widely acknowledged as being pivotal contributors to the advancement of malignant tumours, thus suggesting that the activation of LIMCH1 may play a role in the metabolic reconfiguration of breast cancer cells.

### Association of LIMCH1 expression with the tumour immune microenvironment (TIME)

To evaluate the impact of LIMCH1 on the TIME, we investigated the effectiveness of cancer immunity measures, assessed the presence of immune cells, and analysed the expression of immune checkpoint genes (Fig. 5). Analysis of cancer immunity revealed positive correlations between LIMCH1 expression and scores related to positive cancer antigen presentation, Th22 cell recruitment, Th17 cell recruitment, myeloid-derived suppressor cell (MDSC) recruitment, and negative immune cell infiltration into tumours. Conversely, negative correlations were observed with scores associated with Th1 cell recruitment, NK cell recruitment, Th2 cell recruitment, positive recognition of cancer cells by T cells, and positive killing of cancer cells (Fig. 5A). Consistently, CIBERSORT algorithm estimation of immune cell infiltration revealed that patients with high LIMCH1 expression harboured more protumour immune cells, such as M2 macrophages, and fewer antitumour immune cells, including CD8<sup>+</sup> T cells and NK cells (Fig. 5B). Moreover, increased expression of immune checkpoint-associated genes was observed in the high LIMCH1 group (Fig. 5C).

A comprehensive analysis of the role of LIMCH1 in the TIME was performed by integrating scRNA-seq data with corresponding bulk RNA sequencing data from 24 breast cancer patients (GSE176078) (Fig. 6A). scRNA-seq analysis revealed that LIMCH1 was predominantly expressed in epithelial cells (Fig. 6B, C). In accordance with the stratification of LIMCH1 expression, the cohort of 24 individuals was categorized into high and low LIMCH1 groups by utilizing the median expression level as the delineating threshold (Fig. 6D). Notably, T cells in the high LIMCH1 group exhibited diminished cytotoxic scores in conjunction with elevated exhaustion scores (Fig. 6E). By employing iTalk, which is a computational framework designed for deciphering intercellular interactions via ligand-receptor signal transduction, the analysis yielded a noteworthy discovery. Specifically, among the top 20 significantly altered receptor-ligand pairs between patients categorized into high and low LIMCH1 groups, the upregulated cellular communication pairs primarily involved myeloid cells and their interactions with other cell types (Fig. 6F). Given the substantial involvement of cancer-associated fibroblasts (CAFs) in oncogenic pathways that have been identified via pathway analysis of LIMCH1-related DEGs, including pathways related to focal adhesion, the extracellular matrix, and cell adhesion molecules (Fig. 2), we further examined alterations in pathways associated with CAFs via single-cell sequencing data. Compared with the low LIMCH1 expression group, the high LIMCH1 expression group consistently exhibited activation of pathways that promote cancer cell adhesion and migration, such as focal adhesion and proteoglycans in cancer, as well as activation of oncogenic signalling pathways, including the TNF and TGF $\beta$  pathways (Fig. 6G). This partially explains the upregulation of the TNF and TGF $\beta$  pathways in the high LIMCH1 expression group that was observed via bulk RNA sequencing analysis (Fig. 3A).

These results suggest that high LIMCH1 expression may be involved in mediating immune exhaustion within the TIME of breast cancer.

### Potential of the association of LIMCH1 expression with predicting therapeutic opportunities

Given the evident immunosuppressive TIME characteristics that are associated with high LIMCH1 expression, a subsequent analysis investigated the differences in immunotherapy-predicted pathways between distinct patient subgroups that were categorized as either high or low LIMCH1 expression groups. The results of this analysis revealed a conspicuous trend, with all of the immunotherapy-predicted pathway scores being significantly downregulated within the high LIMCH1 patient group (Fig. 7A). Our investigation further demonstrated that

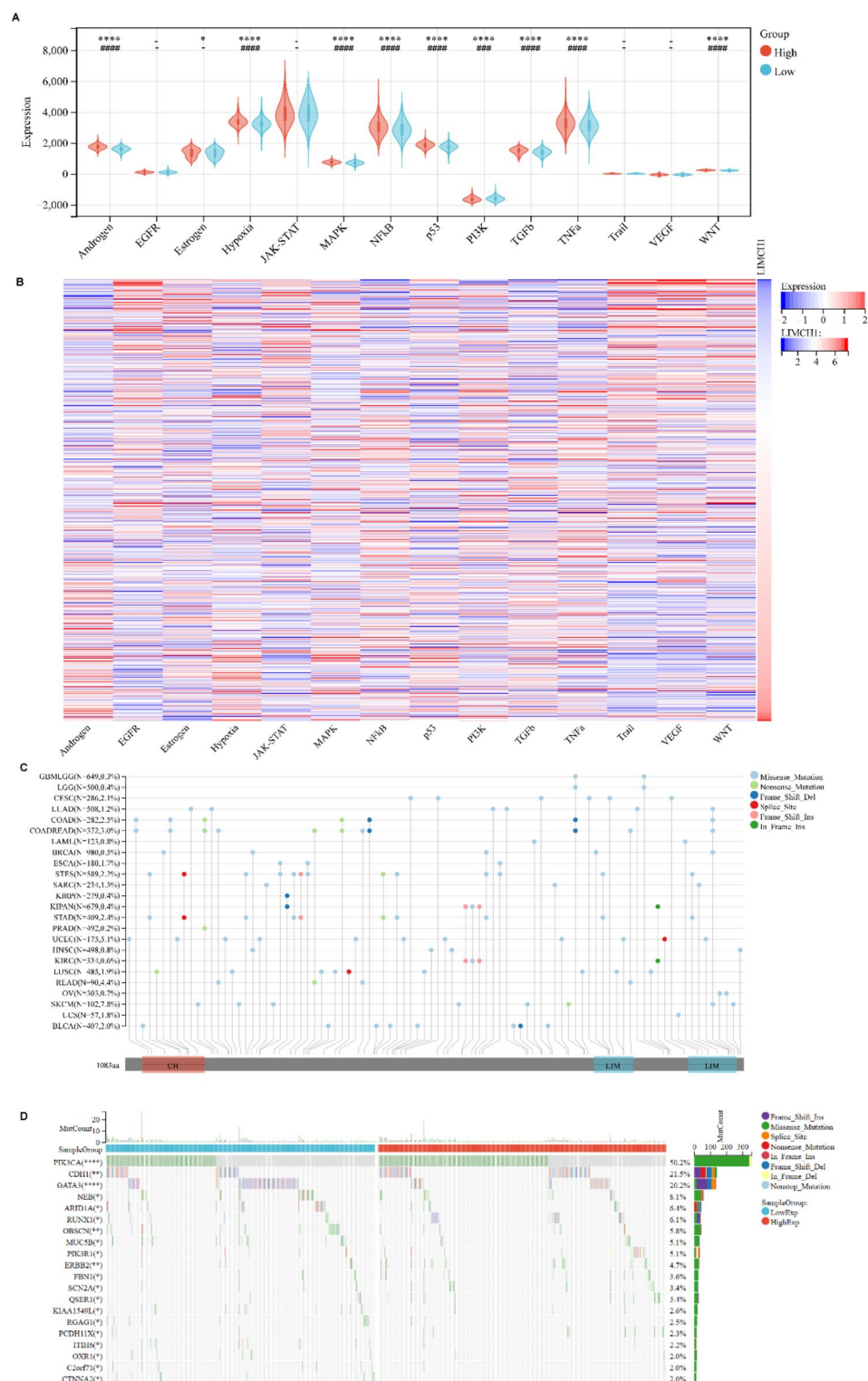


**Fig. 3.** Carcinogenic pathways and mutation landscape comparison. **(A,B)** Differential expression **(A)** and heatmap **(B)** of carcinogenic pathways in groups with high and low LIMCH1. **(C)** Map position of LIMCH1 mutations in pan-cancer. **(D)** Mutation landscape comparison between high and low LIMCH1 groups. Significance indicated as \* $p < 0.05$ , \*\* $p < 0.01$ , \*\*\* $p < 0.001$ , \*\*\*\* $p < 0.0001$ . Power analysis results indicated as # power  $> 0.95$ , ## power  $> 0.99$ , ### power  $> 0.999$ , #### power  $> 0.9999$ .



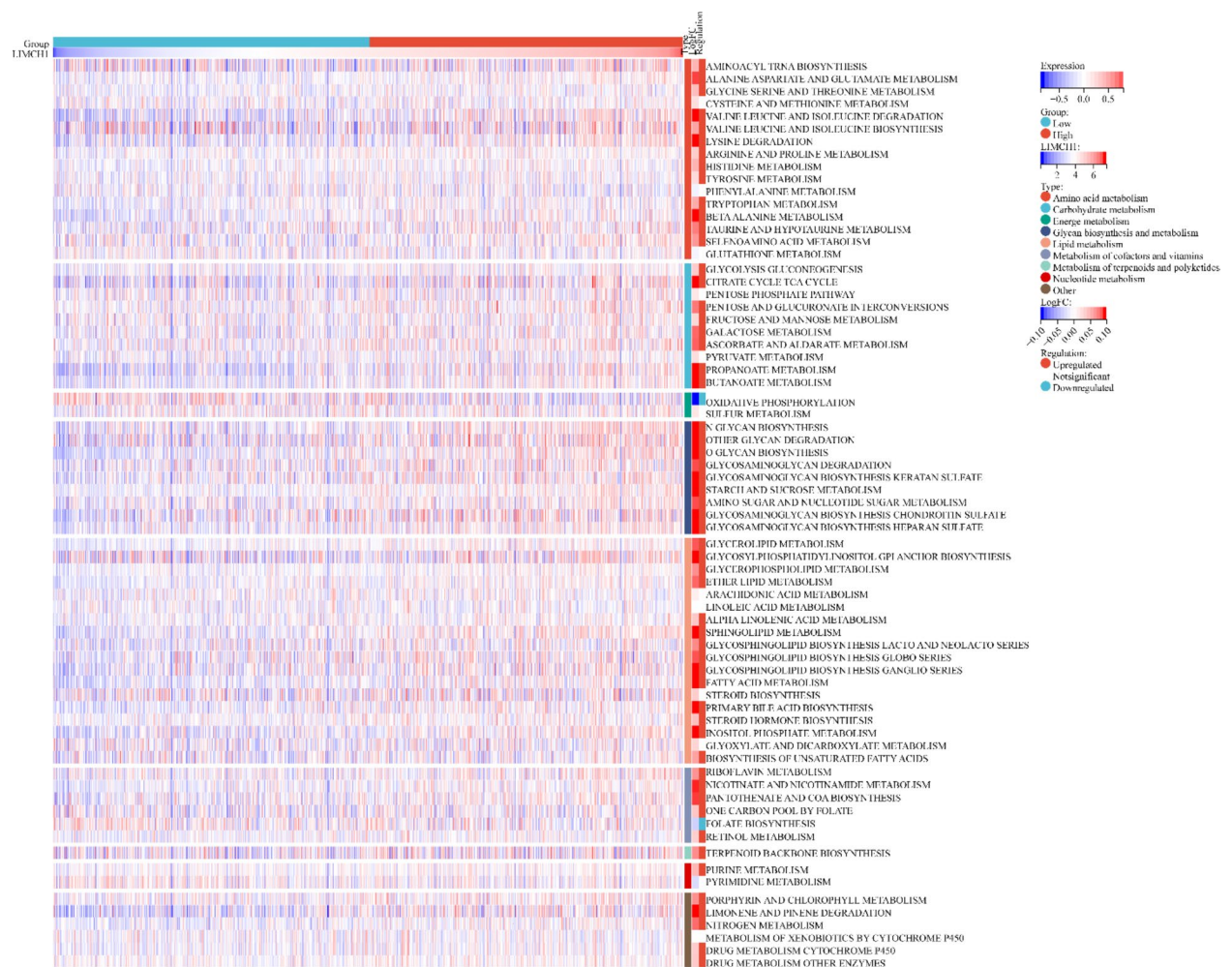


**Fig. 4.** Correlation analysis with breast cancer metabolism. Heatmap displaying expression patterns of metabolism signatures in patients with high and low LIMCH1.

the high LIMCH1 group exhibited elevated scores for immune-suppressive oncogenic pathways, including the Wnt/ catenin network, VEGFA, and hypoxia (Fig. 7B). Additionally, a meticulous assessment of the IC50 values for commonly used breast cancer chemotherapy drugs indicated that the high LIMCH1 group exhibited increased sensitivity to gemcitabine, whereas the low LIMCH1 group demonstrated increased sensitivity to docetaxel and paclitaxel (Fig. 7C).

### Development and validation of the LIMCH1-related nomogram

To develop a pragmatic method for estimating the likelihood of patient survival, we constructed a prognostic nomogram that encapsulates various clinicopathological factors. Based on the insights gained from the Cox analysis, we developed this nomogram to predict the probability of OS (Fig. 8A). Additionally, the calibration plots demonstrated the nomogram's accuracy in predicting survival outcomes with the inclusion of LIMCH1 expression data (Fig. 8B).

### Discussion

In this study, we explored the expression and clinical implications of LIMCH1 in breast cancer. Our results revealed the multifaceted role of LIMCH1 in breast cancer progression, thereby elucidating its connections with clinical characteristics, prognosis, metabolic pathways, the immune microenvironment, and potential therapeutic avenues.

LIMCH1 is a myosin-binding protein that modulates cellular movement by binding to and activating nonmuscle myosin IIA (NMIIA)<sup>24</sup>. Via this interaction, LIMCH1 positively regulates the assembly of actin stress fibres and stabilizes focal adhesions, thus indicating its involvement in the cytoskeletal dynamics that are crucial for cellular function<sup>5,24</sup>. Previous studies have identified LIMCH1 as being both a tumour suppressor and an oncogene in different cancer types, including breast cancer, renal cancer, and lung adenocarcinoma<sup>8,10,25</sup>. Specifically, it has been recognized as being a tumour suppressor in lung cancer<sup>7</sup>, whereas in cervical and breast cancer, it has been implicated as an oncogene<sup>4,11</sup>. However, the precise role of LIMCH1 in tumorigenesis remains to be fully elucidated.

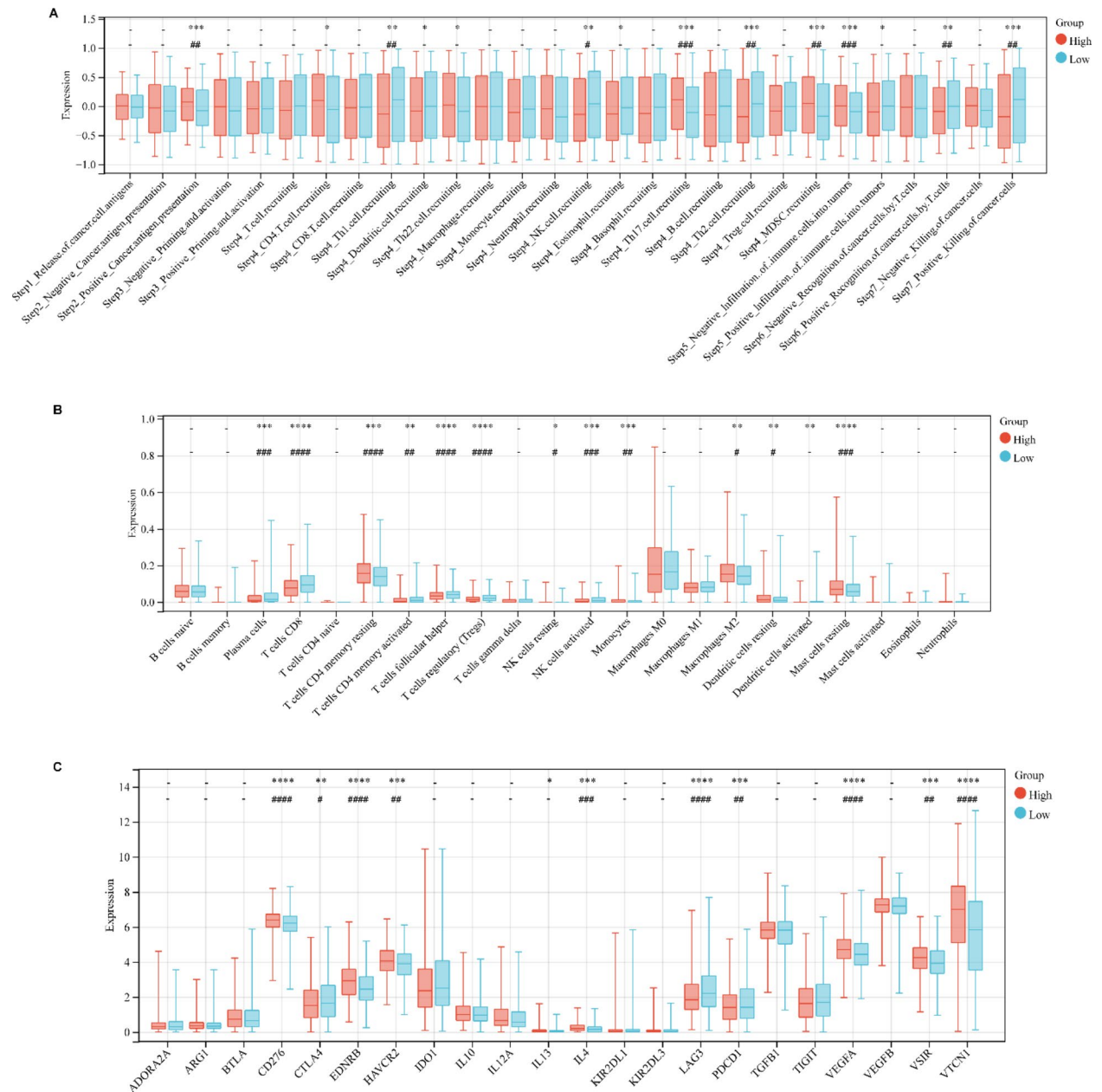


**Fig. 5.** Correlation analysis with TIME. (A–C) Differential expression of (A) immune cycle score, (B) immune cells, and (C) immune checkpoints in high and low LIMCH1 groups. Significance indicated as \* $p < 0.05$ , \*\* $p < 0.01$ , \*\*\* $p < 0.001$ , \*\*\*\* $p < 0.0001$ . Power analysis results indicated as # power  $> 0.95$ , ## power  $> 0.99$ , ### power  $> 0.999$ , #### power  $> 0.9999$ .

Recent advancements in technologies such as transcriptomics, genomics, and bioinformatics have significantly contributed to the discovery of biomarkers, thus offering valuable insights for personalized therapeutic interventions in cancer patients<sup>13,20,23,26</sup>. Our study demonstrated that elevated LIMCH1 expression was associated with unfavourable clinical outcomes and independently predicted prognosis in breast cancer patients. Our results indicated that the high expression of LIMCH1 was associated with the activation of key oncogenic signalling pathways, such as the PI3K-Akt, MAPK, and Wnt pathways, in breast cancer<sup>27–29</sup>. The activation of these pathways may promote the proliferation, survival, and invasive capabilities of breast cancer cells, thereby facilitating tumour progression. Consequently, LIMCH1 may enhance the malignant phenotype of breast cancer cells by influencing these critical cellular signalling pathways. Additionally, when considering the role of LIMCH1 in the organization of the ECM, we speculate that LIMCH1 may be closely associated with the activation and function of CAFs. CAFs promote tumour growth and invasive metastasis by secreting various cytokines and growth factors, such as TGF $\beta$  and HGF<sup>30</sup>. Our study also revealed a correlation between the high expression of LIMCH1 and increased metabolic activity in breast cancer cells. Notably, we observed increased glycolysis and nucleotide metabolism in breast cancer cells with high LIMCH1 expression, which are pathways

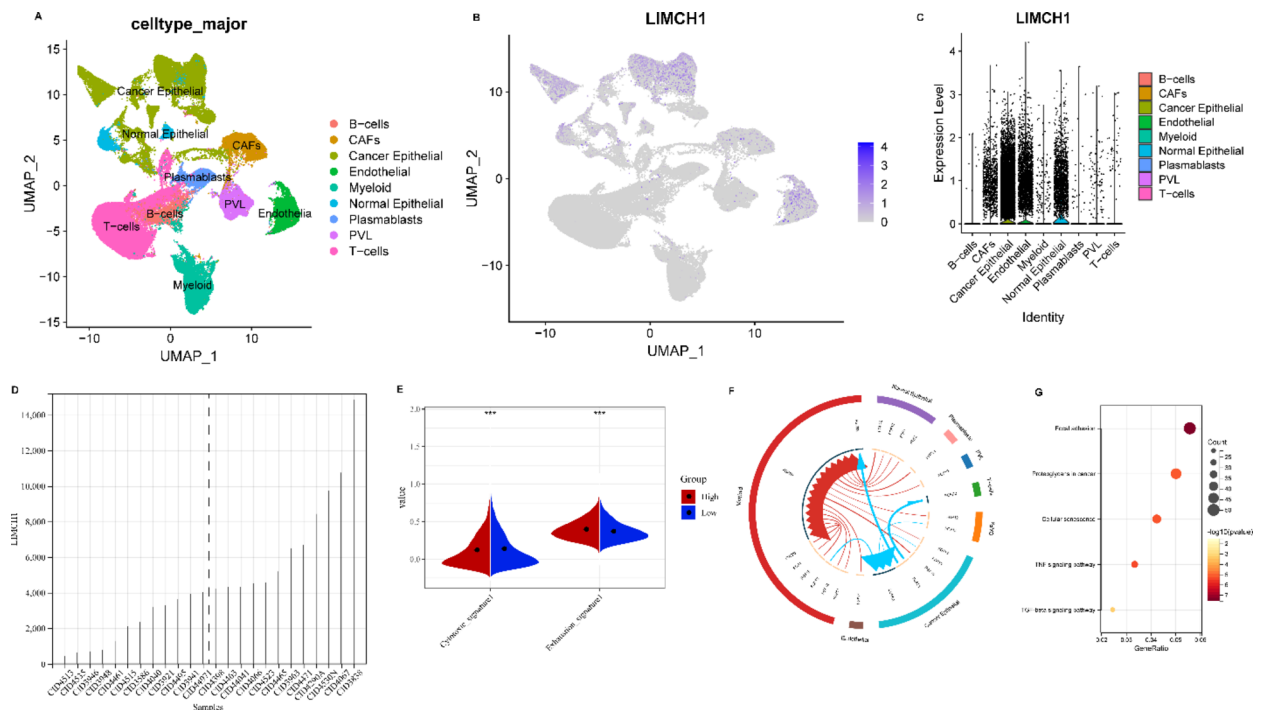


**Fig. 6.** High LIMCH1 indicates an immunosuppressed TIME in scRNA-seq cohort. **(A)** UMAP plot illustrating the composition of 9 main subtypes of breast cancer samples. **(B, C)** Featureplot and Vlnplot depicting the expression of LIMCH1 in the scRNA-seq cohort. **(D)** LIMCH1 distribution in 24 breast cancer samples (divided into 2 patterns). **(E)** Differences in cytotoxic and exhausted T cell scores between high and low LIMCH1 groups. **(F)** Circos plots illustrating ligand-receptor interactions with significant expression differences in the TIME. **(G)** The differential functional analysis of CAFs between groups with high and low LIMCH1 expression was conducted utilizing the KEGG. Significance denoted as \* $p < 0.05$ , \*\* $p < 0.01$ , \*\*\* $p < 0.001$ , \*\*\*\* $p < 0.0001$ .

that are widely recognized as being key contributors to the progression of malignant tumours<sup>31</sup>. These findings suggest that LIMCH1 may play a role in the metabolic reprogramming of breast cancer cells, thus providing the energy and biosynthetic precursors that are necessary for growth and dissemination. Furthermore, the role of LIMCH1 in the TIME indicates that its high expression is associated with an immunosuppressive milieu, thereby potentially facilitating tumour immune evasion by reducing the numbers of CD8<sup>+</sup> T cells and NK cells and increasing the numbers of M2 macrophages. This alteration in the immune microenvironment may further promote the progression of breast cancer and resistance to therapy<sup>32</sup>.

Compared with existing studies<sup>4,25</sup>, our findings provide a comprehensive understanding of LIMCH1 in breast cancer, including its expression patterns, clinical outcomes, genomic alterations, metabolic pathways, and immune microenvironment characteristics. However, given the retrospective nature of this study, prospective clinical trials with larger cohorts are essential for validation. Furthermore, the reliance on digital repositories and clinical specimens highlights the need for external validation through in vitro and in vivo experimentation. Overall, our study highlights LIMCH1 as being a multifaceted molecule that functions in breast cancer pathogenesis, thus emphasizing its potential as a prognostic marker and therapeutic target.

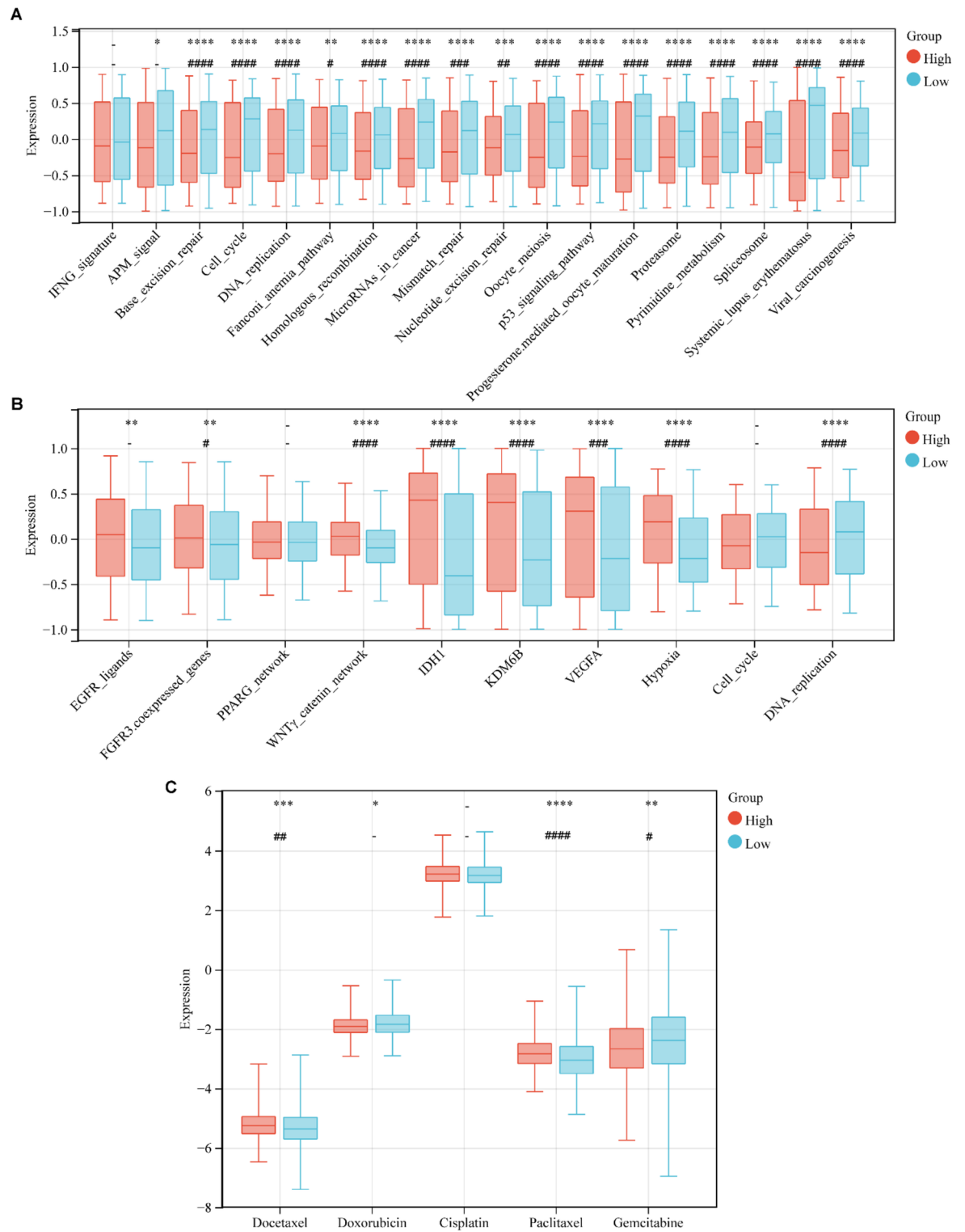


**Fig. 7.** Correlation with therapeutic response in breast cancer. (A–C) Differential expression of (A) immunotherapy-predicted pathways, (B) therapeutic signatures, and (C) IC<sub>50</sub> of chemotherapy drugs in high and low LIMCH1 groups. Significance indicated as \* $p < 0.05$ , \*\* $p < 0.01$ , \*\*\* $p < 0.001$ , \*\*\*\* $p < 0.0001$ . Power analysis results indicated as # power  $> 0.95$ , ## power  $> 0.99$ , ### power  $> 0.999$ , #### power  $> 0.9999$ .



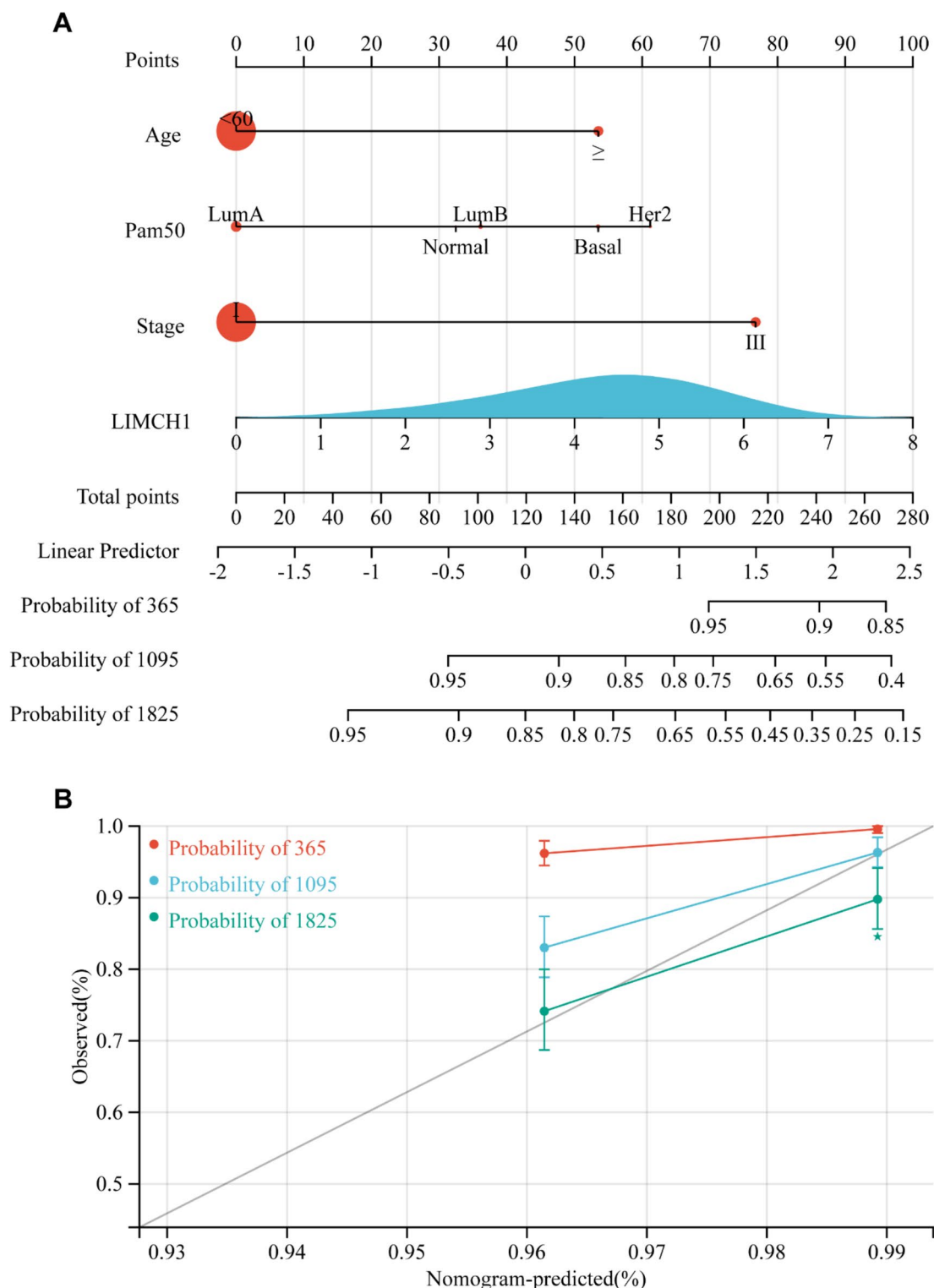


**Fig. 8.** LIMCH1-related nomogram establishment. (A) Nomogram predicting overall survival probability using age, Pam50 subtypes, tumor stage, and LIMCH1 expression. (B) Calibration curves validating prediction accuracy for 1-year (red), 3-year (blue), and 5-year (green) survival predictions.

### Data availability

The raw data of publicly available datasets were downloaded from TCGA dataset (<http://cancer.genome.nih.gov/>) and GEO dataset (<https://portal.gdc.cancer.gov/>). Further inquiries can be directed to the corresponding authors.

Received: 14 February 2024; Accepted: 1 January 2025

Published online: 09 January 2025

# References

1. Siegel, R. L., Miller, K. D., Wagle, N. S. & Jemal, A. Cancer statistics, 2023. *CA Cancer J. Clin.* **73**, 17–48 (2023).
2. Wang, X. et al. Progress of breast cancer basic research in China. *Int. J. Biol. Sci.* **17**, 2069–2079 (2021).
3. Waks, A. G. & Winer, E. P. Breast cancer treatment: a review. *JAMA* **321**, 288–300 (2019).
4. Alifanov, V. V., Tashireva, L. A., Zavyalova, M. V. & Perelmutter, V. M. LIMCH1 as a new potential metastasis predictor in breast cancer. *Asian Pac. J. Cancer Prev.* **23**, 3947–3952 (2022).
5. Penna, M. S., Hu, R. C., Rodney, G. G. & Cooper, T. A. The role of Limch1 alternative splicing in skeletal muscle function. *Life Sci. Alliance* **6**, e202201868 (2023).
6. Zhang, Y., Zhang, Y. & Xu, H. LIMCH1 suppress the growth of lung cancer by interacting with HUWE1 to sustain p53 stability. *Gene* **712**, 143963 (2019).
7. Cao, H. et al. Loss of LIMCH1 predicts poor prognosis in patients with surgically resected lung adenocarcinoma: a study based on immunohistochemical analysis and bioinformatics. *J. Cancer* **12**, 181–189 (2021).
8. Liu, C., Zhang, Y. H., Huang, T. & Cai, Y. Identification of transcription factors that may reprogram lung adenocarcinoma. *Artif. Intell. Med.* **83**, 52–57 (2017).
9. Sewell, W. et al. Cyclical expression of the Notch/Wnt regulator Nrarp requires modulation by Dll3 in somitogenesis. *Dev. Biol.* **329**, 400–409 (2009).
10. Eckel-Passow, J. E. et al. ANKS1B is a smoking-related molecular alteration in clear cell renal cell carcinoma. *BMC Urol.* **14**, 14 (2014).
11. Halle, M. K. et al. A 10-gene prognostic signature points to LIMCH1 and HLA-DQB1 as important players in aggressive cervical cancer disease. *Br. J. Cancer* **124**, 1690–1698 (2021).
12. Zhao, X. et al. CDK6 as a biomarker for immunotherapy, drug sensitivity, and prognosis in bladder cancer: Bioinformatics and immunohistochemical analysis. *Int. J. Med. Sci.* <https://doi.org/10.7150/ijms.101043> (2024).
13. Guo, X. et al. A novel glycolysis-related signature for predicting the prognosis and immune infiltration of uveal melanoma. *Ophthalmic Res.* **66**, 692–705 (2023).
14. Liu, S. Q. et al. Single-cell analysis of white adipose tissue reveals the tumor-promoting adipocyte subtypes. *J. Transl. Med.* **21**, 470 (2023).
15. Shen, W. et al. Sangerbox: A comprehensive, interaction-friendly clinical bioinformatics analysis platform. *iMeta* **1**, e36 (2022).
16. Yu, X. et al. Identification of UCP1 and UCP2 as potential prognostic markers in breast cancer: a study based on immunohistochemical analysis and bioinformatics. *Front. Cell Dev. Biol.* **10**, 12 (2022).
17. Yu, X., Li, W., Sun, S. & Li, J. DDIT3 is associated with breast cancer prognosis and immune microenvironment: an integrative bioinformatic and immunohistochemical analysis. *J. Cancer* **15**, 3873–3889 (2024).
18. Wang, Y., Li, L., Zhang, W., Zhang, G. & Circular RNA circLDB2 functions as a competing endogenous RNA to suppress development and promote cisplatin sensitivity in non-squamous non-small cell lung cancer. *Thorac. Cancer* **12**, 1959–1972 (2021).
19. Hänzelmann, S., Castelo, R. & Guinney, J. GSEA: gene set variation analysis for microarray and RNA-seq data. *BMC Bioinform.* **14**, 7 (2013).
20. Yu, X., Li, W., Sun, S. & Li, J. Investigating the prognostic value of mTORC1 signaling in bladder cancer via bioinformatics evaluation. *Sci. Rep.* **13**, 22066 (2023).
21. Yu, X. et al. The prognostic value of hedgehog signaling in bladder cancer by integrated bioinformatics. *Sci. Rep.* **13**, 6241 (2023).
22. Xu, L. et al. TIP: a web server for resolving tumor immunophenotype profiling. *Cancer Res.* **78**, 6575–6580 (2018).
23. Li, W., Guo, X., Chen, C. & Li, J. The prognostic value of arachidonic acid metabolism in breast cancer by integrated bioinformatics. *Lipids Health Dis.* **21**, 103 (2022).
24. Lin, Y. H. et al. LIMCH1 regulates nonmuscle myosin-II activity and suppresses cell migration. *Mol. Biol. Cell* **28**, 1054–1065 (2017).
25. Cizkova, M. et al. Gene expression profiling reveals new aspects of PIK3CA mutation in ERalpha-positive breast cancer: major implication of the wnt signaling pathway. *PLoS ONE* **5**, e15647 (2010).
26. Cortés-Ciriano, I., Gulhan, D. C., Lee, J. J. K., Melloni, G. E. M. & Park, P. J. Computational analysis of cancer genome sequencing data. *Nat. Rev. Genet.* **23**, 298–314 (2022).
27. Miricescu, D. et al. PI3K/AKT/mTOR signaling pathway in breast cancer: from molecular landscape to clinical aspects. *Int. J. Mol. Sci.* **22**, 173 (2020).
28. Khojasteh Poor, F. et al. Mini review: the FDA-approved prescription drugs that target the MAPK signaling pathway in women with breast cancer. *Breast Dis.* **40**, 51–62 (2021).
29. Xu, X., Zhang, M., Xu, F. & Jiang, S. Wnt signaling in breast cancer: biological mechanisms, challenges and opportunities. *Mol. Cancer* **19**, 165 (2020).
30. D, H. et al. Cancer-associated fibroblasts in breast cancer: challenges and opportunities. *Cancer Commun. (London England)* **42** (2022).
31. Wu, Q., Yu, X., Li, J., Sun, S. & Tu, Y. Metabolic regulation in the immune response to cancer. *Cancer Commun. (Lond.)* **41**, 661–694 (2021).
32. de Visser, K. E. & Joyce, J. A. The evolving tumor microenvironment: from cancer initiation to metastatic outgrowth. *Cancer Cell* **41**, 374–403 (2023).

# Acknowledgements

The authors thank professional English editor (Springer Nature Author Services) for assistance in improving the quality of language.

# Author contributions

Conceptualization: SS, JL and JY. Funding acquisition: BL and WL. Investigation: XY, BL and WL. Project administration: SS, JL and JY. Supervision: SS, JL and JY. Validation: XY, BL and WL. Original draft writing: XY, BL and WL. Writing-review and editing: All authors. All authors have read and agreed to the published version of the manuscript.

# Funding

This work was also supported by a Research Foundation of Shanghai Artemed Hospital (Grant No: AT-M2022YJ01) to Dr. Wenge Li. This work was also supported by a National Natural Science Foundation of China (NSFC) Grant (Grant No: 82303284) to Dr. Bei Li.

## Declarations

### Competing interests

The authors declare no competing interests.

### Ethical declaration and consent to participate

This article does not contain any studies with animals performed by any of the authors. The studies involving human participants were reviewed and approved by The Ethics Committee of Renmin Hospital of Wuhan University (No. WDRY2021-KS009). Written informed consent was obtained from the individual(s) for the publication of any data included in this article.

### Additional information

**Supplementary Information** The online version contains supplementary material available at <https://doi.org/10.1038/s41598-025-85255-0>.

**Correspondence** and requests for materials should be addressed to J.Y., S.S. or J.L.

**Reprints and permissions information** is available at [www.nature.com/reprints](http://www.nature.com/reprints).

**Publisher's note** Springer Nature remains neutral with regard to jurisdictional claims in published maps and institutional affiliations.

**Open Access** This article is licensed under a Creative Commons Attribution-NonCommercial-NoDerivatives 4.0 International License, which permits any non-commercial use, sharing, distribution and reproduction in any medium or format, as long as you give appropriate credit to the original author(s) and the source, provide a link to the Creative Commons licence, and indicate if you modified the licensed material. You do not have permission under this licence to share adapted material derived from this article or parts of it. The images or other third party material in this article are included in the article's Creative Commons licence, unless indicated otherwise in a credit line to the material. If material is not included in the article's Creative Commons licence and your intended use is not permitted by statutory regulation or exceeds the permitted use, you will need to obtain permission directly from the copyright holder. To view a copy of this licence, visit <http://creativecommons.org/licenses/by-nc-nd/4.0/>.

© The Author(s) 2025